The polymorphism L412F in *TLR3* inhibits autophagy and is a marker of severe COVID-19 in males

Susanna Croci, Mary Anna Venneri, Stefania Mantovani, Chiara Fallerini, Elisa Benetti, Nicola Picchiotti, Federica Campolo, Francesco Imperatore, Maria Palmieri, Sergio Daga, Chiara Gabbi, Francesca Montagnani, Giada Beligni, Ticiana D.J. Farias, Miriam Lucia Carriero, Laura Di Sarno, Diana Alaverdian, Sigrid Aslaksen, Maria Vittoria Cubellis, Ottavia Spiga, Margherita Baldassarri, Francesca Fava, Paul J. Norman, Elisa Frullanti, Andrea M. Isidori, Antonio Amoroso, Francesca Mari, Simone Furini, Mario U Mondelli, GEN-COVID multicenter study, Mario Chiariello, Alessandra Renieri & Ilaria Meloni

View supplementary material

Published online: 29 Dec 2021.

Submit your article to this journal

Article views: 1927

Taylor & Francis
Taylor & Francis Group

BRIEF REPORT

OPEN ACCESS   Check for updates

The polymorphism L412F in *TLR3* inhibits autophagy and is a marker of severe COVID-19 in males

Susanna Croci[1,2], Mary Anna Venneri[3], Stefania Mantovani [4], Chiara Fallerini[1,2], Elisa Benetti[2], Nicola Picchiotti[5,6], Federica Campolo[3], Francesco Imperatore[7,8], Maria Palmieri[1,2], Sergio Daga[1,2], Chiara Gabbi[9], Francesca Montagnani[2,10], Giada Beligni[1,2], Ticiana D.J. Farias[11], Miriam Lucia Carriero[1,2], Laura Di Sarno[1,2], Diana Alaverdian[1,2], Sigrid Aslaksen[12], Maria Vittoria Cubellis[13], Ottavia Spiga [14], Margherita Baldassarri[1,2], Francesca Fava[1,2], Paul J. Norman[11], Elisa Frullanti[1,2], Andrea M. Isidori [3], Antonio Amoroso[15,16], Francesca Mari[1,2,17], Simone Furini[2], Mario U Mondelli [4,18], GEN-COVID multicenter study[1], Mario Chiariello[7,8], Alessandra Renieri [1,2,17], and Ilaria Meloni[1,2]

[1]Medical Genetics, University of Siena, Siena, Italy; [2]Med Biotech Hub and Competence Center, Department of Medical Biotechnologies, University of Siena, Siena, Italy; [3]Department of Experimental Medicine, Sapienza University of Rome, Rome, Italy; [4]Division of Clinical Immunology and Infectious Diseases, Department of Medicine, Fondazione IRCCS Policlinico San Matteo, Pavia, Italy; [5]DIISM-SAILAB, University of Siena, Siena, Italy; [6]Department of Mathematics, University of Pavia, Pavia, Italy; [7]Istituto per lo Studio, la Prevenzione e la Rete Oncologica (ISPRO), Core Research Laboratory, Via Fiorentina, Siena, Italy; [8]Consiglio Nazionale delle Ricerche, Istituto DI Fisiologia Clinica, Siena, Italy; [9]Department of Biosciences and Nutrition, Karolinska Institutet, Stockholm, Sweden; [10]Department of Medical Sciences, Infectious and Tropical Diseases Unit, Azienda Ospedaliera Universitaria Senese, Siena, Italy; [11]Division of Biomedical Informatics and Personalized Medicine, and Department of Immunology and Microbiology, University of Colorado Anschutz Medical Campus, Aurora, Colorado, USA; [12]Department of Clinical Science, Universty of Bergen and K.G. Jebsen Center for Autoimmune Diseases, University of Bergen, Bergen, Norway; [13]Department of Biology, Università Degli Studi di Napoli "Federico II", Napoli, Italy; [14]Department of Biotechnology, Chemistry and Pharmacy, University of Siena, Siena, Italy; [15]Department of Medical Sciences, University of Turin, Turin, Italy; [16]Immunogenetics and Transplant Biology, Azienda Ospedaliera Universitaria Città della Salute e della Scienza di Torino, Italy; [17]Genetica Medica, Azienda Ospedaliero-Universitaria Senese, Italy; [18]Department of Internal Medicine and Therapeutics, University of Pavia, Pavia, Italy

ABSTRACT
The polymorphism L412F in TLR3 has been associated with several infectious diseases. However, the mechanism underlying this association is still unexplored. Here, we show that the L412F polymorphism in TLR3 is a marker of severity in COVID-19. This association increases in the sub-cohort of males. Impaired macroautophagy/autophagy and reduced TNF/TNFα production was demonstrated in HEK293 cells transfected with TLR3^{L412F}-encoding plasmid and stimulated with specific agonist poly(I:C). A statistically significant reduced survival at 28 days was shown in L412F COVID-19 patients treated with the autophagy-inhibitor hydroxychloroquine (p = 0.038). An increased frequency of autoimmune disorders such as co-morbidity was found in L412F COVID-19 males with specific class II HLA haplotypes prone to autoantigen presentation. Our analyses indicate that L412F polymorphism makes males at risk of severe COVID-19 and provides a rationale for reinterpreting clinical trials considering autophagy pathways.

Abbreviations: AP: autophagosome; AUC: area under the curve; BafA1: bafilomycin A1; COVID-19: coronavirus disease-2019; HCQ: hydroxychloroquine; RAP: rapamycin; ROC: receiver operating characteristic; SARS-CoV-2: severe acute respiratory syndrome coronavirus 2; TLR: toll like receptor; TNF/TNF-α: tumor necrosis factor

Introduction

In December 2019, a new virus was isolated in Wuhan, China, which was called Severe Acute Respiratory Syndrome Coronavirus 2 (SARS-CoV-2). SARS-CoV-2 is an enveloped positive-sense RNA virus that caused a new pandemic, which WHO named COVID-19 (coronavirus disease-2019).

To date, many characteristics of SARS-CoV-2 are still unclear and, although its ability to be transmitted from one person to another has been ascertained, uncertainties remain about the exact modes of transmission and pathogenicity. In addition, a high variability of symptoms in infected patients

and between different populations has been reported; one of the possible explanations of such variability is the genetic background of the host that may affect immune responses to the virus. Among host genetic factors that might impact on symptoms severity there are genes involved in virus entry and mediators of innate immunity [1,2]. TLRs (toll like receptors) are a class of proteins that play a key role in host innate immunity, causing the production of pro-inflammatory cytokines (TNF, IL1, and IL6) and type I and II Interferons, that are responsible for innate antiviral responses. Among TLR genes, *TLR3* encodes an interferon-inducing dsRNA sensor,

whose activation is involved in protection against different RNA viruses [2–4]. Upon viral infection, TLR3 signaling leads to the activation of two factors, NFKB and IRF3 (interferon regulatory factor 3), which play an essential role in the immune response. This results in the production of various cytokines, including TNF (tumor necrosis factor), activating immune responses. However, increased inflammatory responses can make the patient more susceptible to pneumonia and autoimmune diseases. Accordingly, a protective effect against fatal pneumonia has been reported in the absence of TLR3 [5–7]. Among TLR3 variants, the functional L412F polymorphism (rs3775291; c.1234 C > T) is known to decrease TLR3 expression on the cell surface [8]. This polymorphism also leads to poor recognition of SARS-CoV-2 dsRNA, during replication, compared to its wild-type (WT) counterpart [9] and has been recently associated with SARS-CoV-2 susceptibility and mortality [10].

There is evidence that TLR3, as with other TLRs, acts through autophagy in determining susceptibility to infections [11]. The autophagic pathway is essential during infection and for molecular processes such as cell maintenance and homeostasis [12,13]. Indeed, autophagy is one of the major cell defense mechanisms against pathogens [14]. A role for autophagy is reported in different studies on other coronaviruses such as the mouse hepatitis virus/MHV and the transmissible gastroenteritis virus/TGEV [15,16]. A role in SARS-CoV-2 infection has also been described [17–19]. In particular, SARS-CoV-2 can inhibit autophagy resulting in accumulation of autophagosomes and inhibition of viral clearance that, together with immune dysfunction and the activation of numerous inflammatory cytokines, leads to a more severe form of COVID-19 [20–22].

To shed light on the mechanisms underlying the diverse susceptibility to COVID-19, we performed a nested-control study within our GEN-COVID cohort, confirming the role of L412F polymorphism in the *TLR3* gene in susceptibility to SARS-CoV-2 and further defining the potential mechanisms by which this effect is exerted.

Results and discussion

Comparing the extreme phenotypes of SARS-CoV-2 infection, severe COVID-19 patients (cases) versus SARS-CoV-2 PCR-positive oligo-asymptomatic subjects (controls), and using LASSO Logistic regression on common bi-allelic polymorphisms from whole-exome sequencing, we identified the L412F polymorphism (rs3775291; c.1234 C > T) in *TLR3* as a severity marker (Figure 1A). The grid search curve of the cross-validation score (Figure 1B) shows a maximum of the regularization parameter in 10. With this calibration setting, the 10-fold cross-validation provides good performances in terms of accuracy (73%), precision (74%), sensitivity (73%), and specificity (73%) as shown in Figure 1C. The confusion matrix is reported in Figure 1D, whereas the receiver operating characteristic (ROC) curve (Figure 1E) provides an area under the curve (AUC) score of 80%.

The L412F polymorphism has an overall allele frequency of about 20%, ranging from 30% in European to 0.88% in African (mainly sub Saharan) populations [8]. It is intriguing

that a relatively COVID-19-free population such as sub Saharan has a very low frequency (0.88%) of this polymorphism and that Asian (26.97%) and European (30.01%) have a much higher frequency. The variant protein with phenylalanine is under-represented on the cell surface, it is not efficiently secreted into the culture medium when expressed as the soluble ectodomain, and it has reduced capability to activate the expression of TLR3-dependent reporter constructs [8]. In order to confirm the role of the polymorphism, we compared individuals showing severe COVID-19 (cases) and those with no sign of the disease (controls). We subdivided patients into two categories, those having the polymorphism in heterozygous or homozygous state and those homozygous for the WT allele. We found that the prevalence of L412F polymorphism is significantly higher in cases compared to controls (p-value 2.8×10^{-2}) (Table 1). The global allele frequency of L412F in our cohort (cases and controls) is 29.38%, comparable to the allele frequency of 29.79% reported in the European (non-Finnish) population in the gnomAD database (https://gnomad.broadinstitute.org/). The identified frequencies were in Hardy-Weinberg equilibrium.

Sex-related differences of TLRs activation following stimulation by viral nucleic acid may be involved in the sex-related variability in response to viral infections [23]. Several rare TLR3 loss of function mutations are known to be linked both to influenza and SARS-CoV-2 virus as well as hyperfunctioning mutations [24,25]. In agreement with these data, when we stratified by gender, the statistically significant difference increased in the sub-cohort of males giving an Odds Ratio of 1.94 (95% confidence interval, 1.23 to 3.06; p = 3.8x10^{-3}), whereas it was lost in the sub-cohort of females (p-value 5.8×10^{-1}) (Tables 1, 2, 3).

We then investigated the prevalence of patients carrying L412F in heterozygous or homozygous states in all 4 categories of COVID-19 clinical severity, considering only male subjects regardless of age (n = 665). We found that the prevalence of carriers directly increased with the severity of COVID-19, from a clinical condition not-requiring hospitalization to intratracheal intubation (Figure 1F)

The L412F substitution in TLR3 falls in the ectodomain, in the 14 leucine-rich repeats/LRR domain, a motif of 22 amino acids in length that folds into a horseshoe shape [26]. Proteins containing leucine-rich repeats are involved in a variety of biological processes, including signal transduction, cell adhesion, DNA repair, recombination, transcription, RNA processing, disease resistance, apoptosis, and the immune response [27]. The L412F substitution is expected to have a limited structural impact with minimal rearrangement of near hydrophobic amino acids such as tryptophan 386 (Figure 2). However, the absence of one of the leucines probably determines a different rearrangement of the motif and consequently of the near glycosylation site Asn414, having an impact on protein-protein interaction and in signal transduction process [28].

Germline knockout of *TLR3* inhibits autophagy and upregulation of TLR3 promotes damage after myocardial infarction mainly because of autophagy rather than inflammatory activation [29]. Interestingly, we could notice a statistically significant (p = 3.8x10^{-2}) reduced survival at 28 days in TLR3_L412F COVID-19 patients treated with
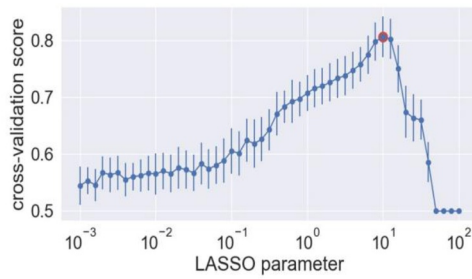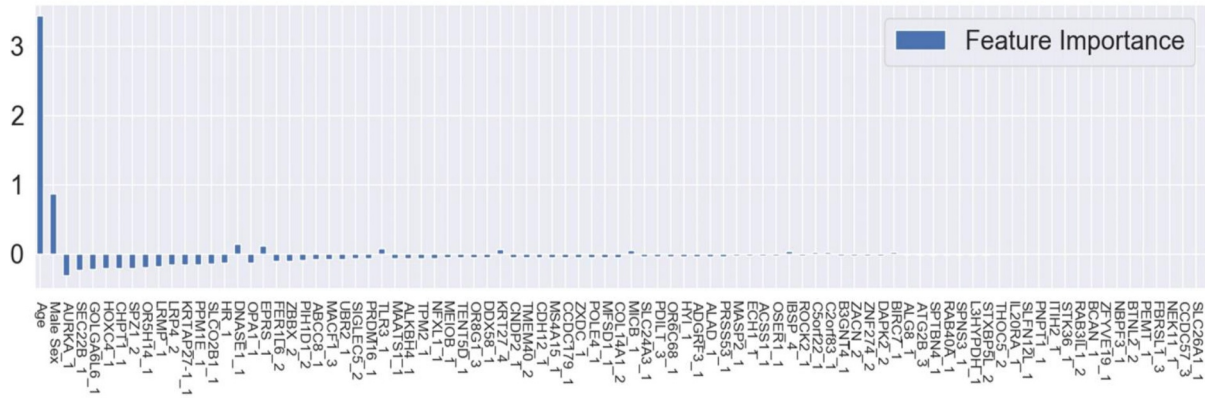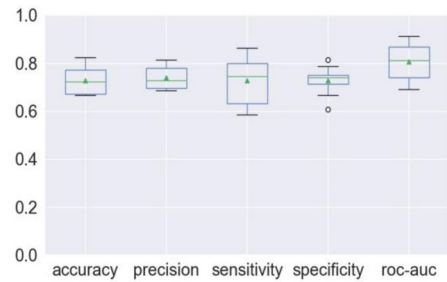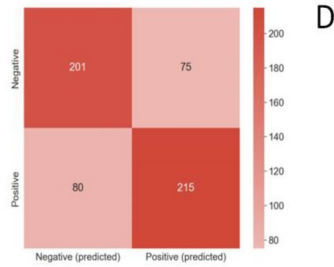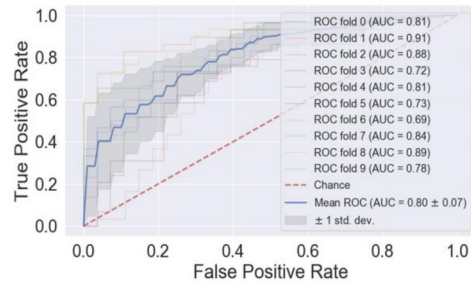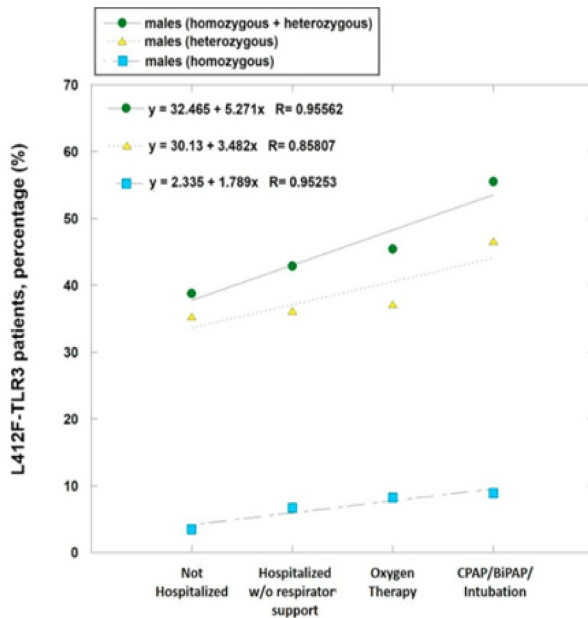
Figure 1. The histogram of the LASSO logistic regression weights represents the importance of each feature for the classification task, (A) The positive weights reflect a susceptible behavior of the features to the target COVID-19 disease, whereas the negative weights a protective action. (B) Cross-validation ROC-AUC score for the grid of LASSO regularization parameters; the error bar is given by the standard deviation of the score within the 10 folds; the optimal regularization parameter is chosen by selecting the one with highest cross-validation score (red point). (C) Boxplot of accuracy, precision, sensitivity, specificity, and ROC-AUC score for the 10-fold of the cross-validation. The box extends from the Q1 to Q3 quartile, with a line at the median (Q2) and a triangle for the average. (D) Confusion matrix for the aggregation of the logistic regression predictions in the 10 folds of the cross-validation. (E) ROC curve for the 10 folds of the cross-validation. (F) Distribution of carriers of the polymorphism L412F in homozygous or heterozygous states stratified by clinical category.

Table 1. L412F and COVID-19 outcome (both sexes).

	Cases	Controls	Marginal Row Totals
L412F	186 (55.0%)	139 (46.3%)	325 (50.9%)
Wild-Type	152 (45.0%)	161 (53.7%)	313 (49.05%)
Marginal Column Totals	338 (52.97%)	300 (47.02%)	638 (Grand Total)

p-value (cases vs controls) = 2.8×10^{-2}

Table 2. L412F and COVID-19 outcome (males only).

	Cases	Controls	Marginal Row Totals
L412F	131 (55.3%)	45 (38.8%)	176 (49.8%)
Wild-Type	106 (44.7%)	71 (61.2%)	177 (50.1%)
Marginal Column Totals	237 (67.13%)	116 (32.86%)	353 (Grand Total)

p-value (cases vs controls) = 3.6×10^{-3}

Table 3. L412F and COVID-19 outcome (females only).

	Cases	Controls	Marginal Row Totals
L412F	55 (54.5%)	94 (51.1%)	149 (5.,3%)
Wild-Type	46 (45.5%)	90 (48.9%)	136 (47.7%)
Marginal Column Totals	101 (35.43%)	184 (64,56%)	285 (Grand Total)

p-value (cases vs controls) = 5.8×10^{-1}

hydroxychloroquine (HCQ) (Figure 3A). As this drug is a well-established inhibitor of autophagy, we reasoned that alterations of this important biological process might have a role in the increased severity of the clinical phenotypes of SARS-CoV-2 infection in patients with the TLR3^{L412F} polymorphism. Notably, beside being entirely ineffective at changing the clinical evolution of COVID-19, which led to retraction of the paper reporting the clinical trial [30], HCQ may have been responsible for reportedly increased fatality rates among patients treated with this drug [31,32]. Poly(I:C) stimulation of the TLR3 receptor has already been shown to stimulate autophagy [29]. Therefore, we decided to compare the efficacy of transfected WT and L412F-mutated receptors in inducing autophagy upon poly(I:C) treatment. To monitor autophagy, we used indirect immunofluorescence microscopy to score the formation of punctate intracellular vacuoles stained for LC3B. Moreover, to better appreciate autophagosomal formation, we also used bafilomycin A$_1$ (Baf A1), an inhibitor of lysosomal acidification, to prevent lysosomal degradation of autophagosome-associated LC3B [33]. Baf A1 allows, in fact, the detection of each autophagosome formed in the time-lapse between addition of the drug to cells and harvesting [33]. Importantly, to avoid potentially confounding effects of the endogenous TLR3 receptor in transfected cells, we used *TLR3* knockout HEK cells. In these cells, when transfected with a plasmid encoding WT TLR3 (TLR3_WT), we observed a progressively increasing number of autophagosomes (APs) when stimulated with poly(I:C) for different time points in the presence of BAF A1 (compared to BAF A1 alone) (Figure 3B-C), indicating a stimulation of the synthesis of these vesicles and a positive autophagic flux. Conversely, in HEK cells transfected with TLR3_L412F, the number of AP was reduced by poly(I:C)

stimulation in the presence of BAF A1 (Figure 3B-C), demonstrating a block in AP synthesis and a reduced autophagic flux. Interestingly, in the absence of BAF A1, AP numbers did not increase upon poly(I:C) stimulation, suggesting that, in HEK cells, fast degradation of AP may compensate for a small increase in the synthesis. Indeed, also rapamycin (RAP), a strong stimulus for autophagy [34], induced only a small increase of AP in the absence of BAF A1 in these cells upon transfection of both TLR3_WT and TLR3_L412F, supporting slow rates of AP synthesis in these cells upon stimulation with different stimuli. The fusion process of autophagosomes with hydrolase-containing lysosomes represents the final step in the degradation process along the autophagic route and its evaluation provides important information for flux analysis [33]. Therefore, as a further confirmation of a reduced autophagic flux in HEK cells expressing the TLR3^{L412F} mutant as compared to TLR3_WT-transfected cells, we decided to score fusion of autophagosomes to lysosomes in these cells upon poly(I:C) stimulation, by measuring colocalization rate of LC3B and LAMP-1, through analysis with the Volocity software of immunocytochemistry experiments (Fig. S1).

During SARS-CoV-2 infection, adipocytes produce proinflammatory cytokines like TNF, IL6 and IL1B/IL-1β which recruit immune cells to the site of infection [35]. Autophagy is stimulated and regulated by these pro-inflammatory cytokines [35]. TNF is a potent immunomodulator and proinflammatory cytokine that has been implicated in the pathogenesis of
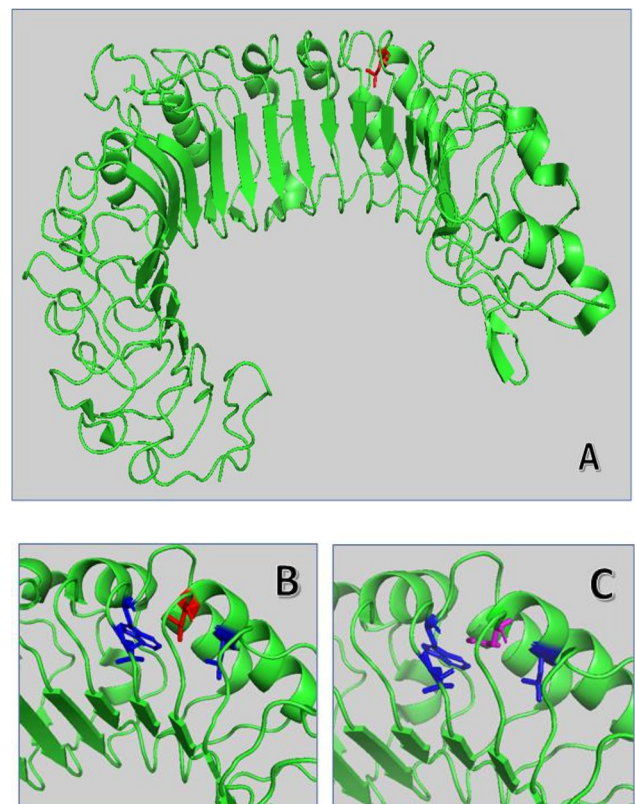

Figure 2. Superposition of wild-type and mutated TLR3 protein. (A) TRL3 human protein tridimensional structure of 2Z7X crystal structure. In green cartoon representation of TLR3 protein. (B) and (C) Zoom of the mutated region with Leu412 in red sticks and Phe412 in magenta. The hydrophobic core of Leu377, Leu389, and Trp386 is in blue sticks.
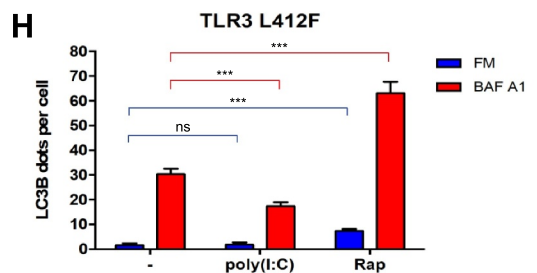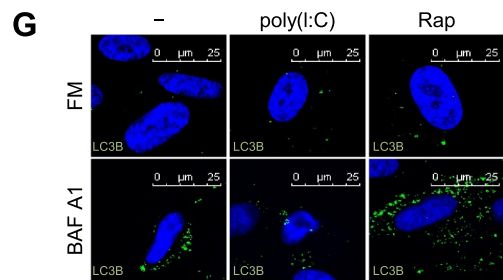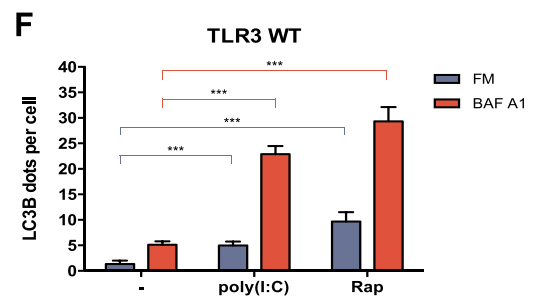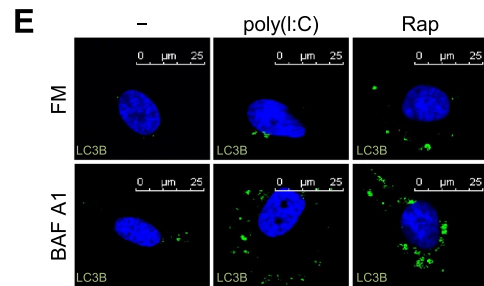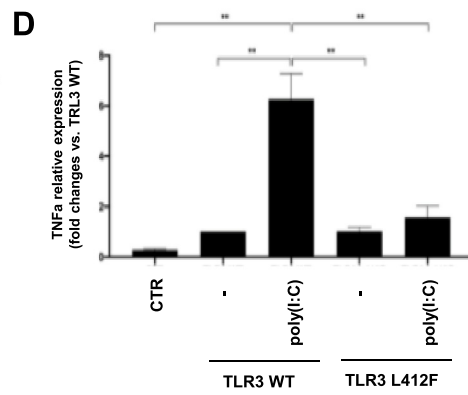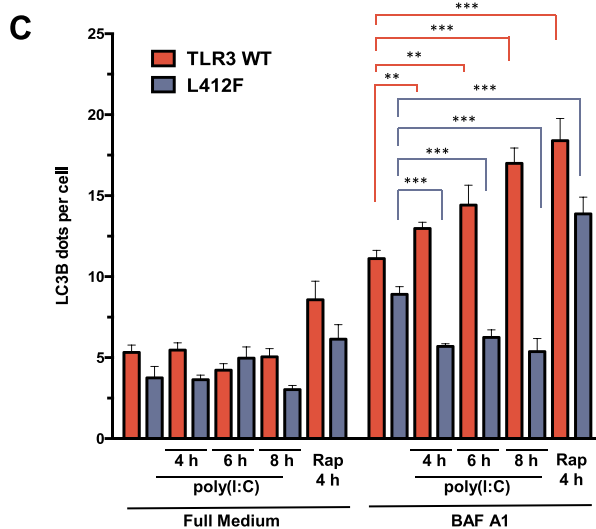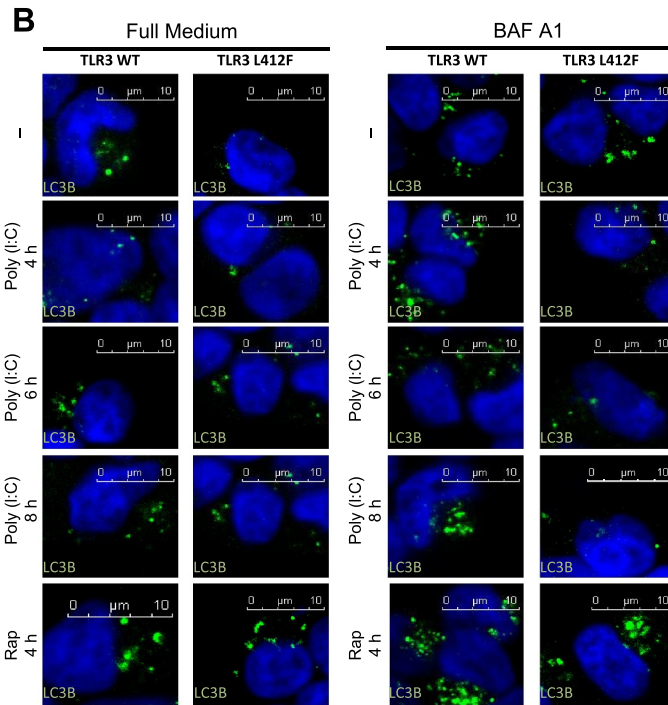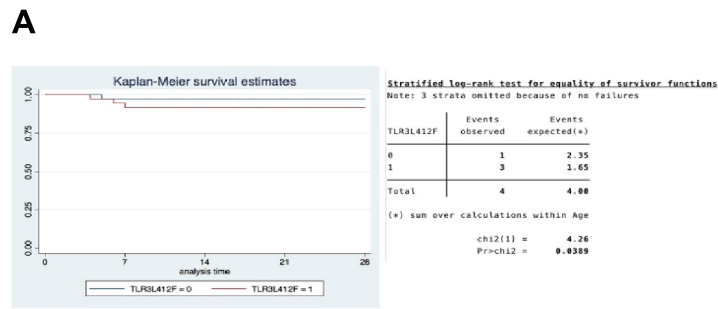
Figure 3. Analysis of autophagy in TLR3_L412F-expressing cells. (A) 28-day survival study of TLR3- L412F carriers vs not-carriers in the group treated with hydroxychloroquine. N = 156, with 73 carriers of TLR3- L412F. Three carriers and 1 not-carrier died in the first 28 days of treatment. (B) Analysis of autophagy in HEK-KO cells expressing wild type or L412F mutant proteins. HEK-KO cells were transfected for 24 h with plasmids encoding TLR3_WT and TLR3_L412F. Cells were next incubated in full medium (FM) or FM + 400 nM bafilomycin A_1 (BAF A1) for 3 h and stimulated for increasing times with 50 μg/ml poly(I:C), as indicated. Cells were next fixed, permeabilized with 100 μg/ml digitonin and stained with anti-LC3B antibodies and revealed with Alexa Fluor 488-conjugated secondary antibodies. Nuclei were stained with DAPI. Where indicated, RAP (500 nM, for 2 h) was used as positive control for induction of autophagy. (C) Same as in B, but the amount of autophagosomes (scored as LC3B-positive dots) per cell was quantified by Volocity software. Measures were obtained by analyzing at least 400 cells/sample from 3 different experiments (n = 3). (D) Analysis of *TNF* mRNA expression in HEK-KO cells expressing wild type or L412F mutant proteins. HEK-KO cells were transfected for 24 h with plasmids encoding empty vector (CTR), TLR3_WT and TLR3_L412F and next stimulated for increasing times with 50 μg/ml poly(I:C), where indicated. TNF

levels were evaluated by Real Time PCR. The gene expression levels were evaluated by the fold change versus TLR2 WT sample using the equation 2^{-DDCt}. Data are presented as the mean ± SEM. Data significance was analyzed using One-way ANOVA test with Holm-Sidak's correction. Asterisks were attributed for the following significance values: P > 0.05 (ns), P < 0.05 (*) and P < 0.01 (**). (E) Normal human fibroblasts (NDHF) from subjects expressing the TLR3_WT receptor were stimulated with 50 μg/ml poly(I:C) or RAP (1 μ M) for 4 h, in full medium alone or containing 400 nM bafilomycin A$_1$ for 3 h. Cells were next fixed, permeabilized with 100 μg/ml digitonin and stained with anti-LC3B antibodies and revealed with Alexa Fluor 488-conjugated secondary antibodies. Nuclei were stained with DAPI. (F) Same as in E, but the number of autophagosomes (scored as LC3B-positive dots) per cell was evaluated for each sample by Volocity software. (G and H) same as in E-F, but fibroblasts are homozygous for the TLR3_L412F receptor. Statistical analysis was performed using Student's t test. Means § SEM for each value are shown in the graphs. ns = not significant; ** = p < 0.01; *** = p < 0.001. < 0.001.

autoimmune and infectious diseases. It is produced by activated monocytes and macrophages, as well as by many other cell types, including lymphocytes, as a transmembrane protein. Through cell modulation, TNF can activate both cell death and survival mechanisms. TNF induces autophagy through a feedback mechanism, causing further recruitment and activation of lymphocytes and contributing to the excess inflammation typical of SARS-CoV-2 infection [36]. As chloroquine, a powerful inhibitor of autophagy, inhibits production of different cytokines, among which TNF [37], we next decided to test if the inhibitory effect of the L412F mutation on autophagy was also able to mimic the effect of the pharmacological inhibitor of this process in HEK cells. Indeed, while poly(I:C) readily stimulated TNF expression in HEK cells transfected with the TLR3_WT receptor, this effect was completely abolished in TLR3_L412F-transfected cells (Figure 3D).

In order to validate data obtained on transfected HEK cells, we next isolated and cultured skin fibroblasts from healthy donors with different genotypes relative to the TLR3 locus: wild-type (WT/WT) and L412F (L412F/L412F) homozygous. In these primary fibroblasts, immunofluorescence analysis revealed that the number of LC3B-positive vesicles increased upon poly(I:C) stimulation both in the absence and in the presence of BAF A1 (Figure 3E-F), showing an overall positive autophagic flux in WT cells, while the flux resulted significantly reduced in L412F/L412F fibroblasts (Figure 3G-H). As a control, RAP stimulation of both WT/WT and L412F/L412F showed a positive autophagic flux (Figure 3(E,F,G,H) confirming that the mutation specifically affected TLR3-dependent autophagy and not the general autophagic process. Also in these cells, we confirmed a reduced autophagic flux in TLR3_L412F-expressing fibroblasts as compared to TLR3_WT-expressing cells, upon stimulation with poly(I:C), by measurement of the LC3B-LAMP1 colocalization rate (Fig. S2).

Overall, our results therefore suggest that the outcome of clinical trials with HCQ should be reinterpreted in the light of TLR3^{L412F} polymorphism status. Negative effects of the drug in L412F bearing subjects may have masked a possible positive outcome in L412F-free subjects. Importantly, they also support a positive role of autophagy in the anti-viral response of the organism to SARS-CoV-2, as suggested by a recent report by Hayn and colleagues [38], demonstrating that at least 3 viral proteins are able to specifically block autophagic turnover.

TLR3 variant L412F has been associated with a wide range of autoimmune diseases including Addison disease and hypothyroidism [39]. TLR3 rare variants resulting in partial loss of function and occurring together with the common variant L412F, or with another rare variant, have been identified in Addison disease [40]. Persistent viral infections in

a background of defective innate immunity lead to overexpression of HLA allotypes prone to present autoantigen. Defects of autophagy have been observed in many infectious and autoimmune diseases. Alteration of autophagic processes causes the onset of autoimmunity due to increased survival and reduced apoptosis of self-reactive lymphocytes [41–43]. HLA has been shown to be implicated in disease severity and clinical outcome of patients with COVID-19 [44]. Accordingly, an increased frequency of autoimmune disorders as co-morbidity was found in our cohort in L412F COVID-19 patients with specific HLA class II haplotypes prone to autoantigen presentation. In particular, we analyzed the DR3-DQ2 haplotype which predisposes to different types of autoimmune diseases [45,46]. The frequency of autoimmune disorders is indeed significantly increased in male patients with HLA DR3/DQ2 haplotype and L412F, especially diabetes (25%) (Table 4 and Table 5). These results suggest that the combination of L412F in TLR3 and a specific class II HLA haplotype puts male patients at risk of post-COVID autoimmune exacerbation emphasizing the need for appropriate follow-up.

No association was found between AIRE loss of function variants and COVID-19 outcome, as outlined by the absence of the gene in Figure 1.

In conclusion, we have identified the second protein-encoding polymorphism that modulates COVID-19 outcome. These results indicate that L412F polymorphism in the TLR3 gene makes males, in whom after puberty testosterone lowers TLR3 expression, at risk of severe COVID-19 in a context of a polygenic model. Moreover, based on impairment of autophagy, these data provide a rationale for reinterpreting clinical trials with HCQ stratifying patients by L412F. Finally, the combination of L412F in TLR3 and specific HLA class II haplotypes may put male patients at risk of post-acute sequelae of SARS-CoV-2 infection pointing to the need for an appropriate follow-up. Our experiments suggest an important role of autophagy downstream of the TLR3 receptor, possibly affecting TNF production and susceptibility to infections, including SARS-CoV-2, pinpointing to IFNs treatment (especially IFN γ) avoiding hydroxiclorochine.

Table 4. Association between DR3-DQ2 + L412F haplotype and autoimmune disorders in male patients.

	With autoimmune disease	W/O autoimmune disease	Marginal Row Totals
DR3-DQ2 + L412F	12 (3.59%)	12 (3.59%)	24 (7.18%)
Other	64 (19.16%)	246 (73.65%)	310 (92.81%)
Marginal Column Totals	76 (22.75%)	258 (77.24%)	334 (Grand Total)

p-value (cases vs controls) = 0.000951

Table 5. Male patients with L412F and HLA DR3/DQ2 haplotype.

PatientID	Age	Ethnicity (white = 1, hispanic = 4)	Clinical Category	GT TLR3 (L412F)	Clinical known comorbidities
AR-COV-25	69	1	4	0/1	Hypertension, Kidney failure, COLD
BS-COV-102	59	1	3	0/1	Diabetes Mellitus, diabetic neuropathy with transmetarsal amputation, bilateral fachiectomy, left hernioplasty, diabetic retinopathy
BS-COV-58	47	1	3	0/1	Hypertension
BS-COV-65	72	1	2	0/1	Rheumatoid Arthritis
BS-COV-70	65	1	3	0/1	Autoimmune hepatitis, autoimmune polyghiandol syndrome, previous autoimmune thyroid
CR-COV-17	61	1	2	0/1	Inflammatory disease, Hypertension
CR-COV-4	66	1	3	0/1	None
LS-COV-10	37	1	1	0/1	DLB-CL EBV+, Immunodeficiency, Bipolar Disorder
LS-COV-19	58	4	2	0/1	Diabetes Mellitus
LS-COV-8	48	1	4	0/1	Hypertension
MORE-COV-16	65	1	3	0/1	Hypertension, Asthma, Dyslipidemia
MORE-COV-7	72	1	4	0/1	Hypertension
PG-COV-15	87	1	2	0/1	Congestive heart failure, Dyslipidemia, Stroke
PG-COV-23	68	1	1	0/1	N/A
PV-COV-02	65	1	2	0/1	Rheumatoid Arthritis
PV-COV-23	72	1	3	0/1	Hypertension, Diabetes Mellitus
PV-COV-24	79	1	2	0/1	Atrial Fibrillation, Diabetes Mellitus, Kidney failure
PV-COV-39	33	4	4	0/1	Diabetes Mellitus, Obesity
PV-COV-73	54	1	3	0/1	None
PV-COV-97	66	1	4	0/1	Congestive Heart Failure, Hypertension, Diabetes Mellitus
RUF-COV-1	52	1	0	0/1	None
SPC-COV-14	56	1	3	0/1	Asthma, HCV
TV-COV-81	44	1	1	0/1	None
TV-COV-96	51	1	2	0/1	Hypertension

Materials and methods

Patients

We performed a nested case-control study (NCC). We used a cohort of 1319 subjects (cases and controls) from the Italian GEN-COVID Multicenter study, infected with SARS-CoV-2 diagnosed by RT-PCR on nasopharyngeal swab [47]. Cases were defined as patients needing endotracheal intubation or CPAP/biPAP ventilation. Controls were oligo-asymptomatic subjects not requiring hospitalization.

Ethics approval

The GEN-COVID study was approved by the University Hospital of Siena Ethical Review Board (Protocol n. 16,929, dated 16 March 2020).

LASSO logistic regression

We adopted the $\lambda \sum_{k=1}^{p} |\beta_k|$ Least Absolute Shrinkage and Selection Operator (LASSO) logistic regression model for the classification of severe COVID-19 patients (cases) versus SARS-CoV-2 PCR-positive oligo-asymptomatic subjects (controls), able to enforce both the sparsity and the interpretability of the results. By denoting with β_k the coefficients of the logistic regression and by lambda (λ) the strength of the regularization, the LASSO regularization [48] term of the loss, has the effect of shrinking the estimated coefficients to 0. In this way, the weights of the logistic regression algorithm can be interpreted as the feature importances of the subset of the most relevant features for the task [49]. The input features are the common bi-allelic polymorphisms from whole-exome sequencing as well as gender, and the age, the latter as a continuous

variable normalized between 0 and 1. Common bi-allelic polymorphisms are defined as combinations of two polymorphisms, each with minor allele frequency above 1%, with frequency above 5% in the cohort.

The fundamental hyper-parameter of the logistic regression algorithm is the strength of the LASSO term, which is tuned with a grid search method on the average area under the ROC curve for the 10-fold cross-validation. The regularization hyperparameter varies in the range $[10^{-3}, 10^2]$ with 50 equally spaced values in the logarithmic scale. The optimal regularization parameter is chosen by selecting the parameter with the highest cross-validation score. During the fitting procedure, the class slight unbalancing is tackled by penalizing the misclassification of the minority class with a multiplicative factor inversely proportional to the class frequencies. The data preprocessing was coded in Python, whereas for the logistic regression model the scikit-learn module with the liblinear coordinate descent optimization algorithm was used. Performances of the model were evaluated using the cross-validation confusion matrix as well as by computing precision, sensitivity, specificity, and the ROC curve.

Cell culture and transfection

HEK-Dual™ Null (NF/IL8) cells (Invivogen, hkd-nullni) cells were cultured in Dulbecco modified Eagle medium (DMEM; Euroclone, ECB7501L) supplemented with 10% fetal bovine serum (FBS; Euroclone, ECS0180L), 2 mM L-glutamine (Carlo Erba, ABP379-100) and 100 units/ml penicillin-streptomycin (Life Technologies, 15,140,148) at 37°C in an atmosphere of 5% CO_2:air. Transfections were performed with 1 µg DNA plasmid using lipofectamine LTX (Life Technologies, 15,338,500). The cells were seeded to be 70% to 80% confluent, then DNA was diluted in DMEM with 10 mM HEPES, pH 7.2. Lipofectamine LTX was next added

to the complex (5 μl) to allow creation of complexes (30 min at RT). Ultimately, DNA-lipid complexes were added to cells. Bafilomycin A$_1$ was from Santa Cruz Biotechnology (sc-201,550). Human primary fibroblasts were obtained from the Genetic Biobank of Siena (http://biobanknetwork. telethon.it/; cell line number: Rett 2250, 2980/18, 1031/15, Rett 1200). Fibroblasts were cultured in Dulbecco Modified Eagle medium supplemented with 10% FBS, 2% L-glutamine and 1% penicillin-streptomycin, according to standard protocols, and routinely passed 1:2 with trypsin-EDTA (0.05%) solution (Irvine Scientific, 9342).

Immunofluorescence (IF)

Cells were washed with phosphate-buffered saline (PBS; Oxoid, BR0014G), then fixed with 4% paraformaldehyde in PBS for 20 min, washed with PBS and permeabilized with digitonin solution (Life Technologies, BN2006) for 20 min. Then, the cells were washed three times in PBS. Permeabilized cells were incubated with anti-LC3B (MBL, M152–3) and/or anti-LAMP1 (Cell Signaling Technology, 9091) primary antibodies for 1 h, washed three times with PBS, and then incubated with anti-mouse Alexa Fluor 488-conjugated (Life Technologies, A21202) and/or Alexa Fluor 647 (Life Technologies, A21245) secondary antibodies; subsequently cells were washed three times with PBS. Nuclei were stained with a solution of 6 μM of 4′,6-diamidino-2-phenylindole (DAPI; Sigma Aldrich, D9542) in PBS for 10 min. Coverslips were mounted in a fluorescence mounting medium (Dako, S3023). Samples were visualized on a TSC SP5 confocal microscope (Leica Microsystems, 5,100,000,750) installed on an inverted LEICA DMI 6000CS (Leica Microsystems, 10,741,320) microscope and equipped with an oil immersion PlanApo 63 × 1.4 NA objective. Images were acquired using the LAS AF acquisition software (Leica Microsystems, 10,210). Poly(I:C) was from InvivoGen (31,852–29-6).

Dot count and statistical analysis for autophagy

For the LC3B-positive dot counts, we performed intensito-metric analysis of fluorescence using the Quantitation Module of Volocity software (PerkinElmer Life Science). LC3B-LAMP 1 colocalization rate was measured by the Quantification tool of LAS AF software (Leica Microsystems). Dot counts and colocalization rate were subjected to statistical analysis. Measures were obtained by analyzing at least 400 cells/sample (dot counts) or 250 cells/sample (colocalization rate) from 3 different experiments. Significance (P value) was assessed by Student's t test, using GraphPad Prism6 software. Asterisks were attributed for the following significance values: P > 0.05 (ns), P < 0.05 (*), P < 0.01 (**), P < 0.001 (***).

Real time qPCR analysis of TNF expression

Total RNA was isolated using the RNAeasy Mini Kit (Qiagen, NC9677589) according to the manufacturer's instructions. cDNA synthesis was performed using the Maxima First Strand cDNA Synthesis Kit (Life Technologies, EP0751). Neo-synthetized cDNA was used to perform Real Time PCR using the PowerUp Sybr Green (Life Technologies, A25779). The following primers were used: *TNF* Fw CTATCTGGGA GGGGTCTTCC; *TNF* Rw GGTTGAGGGTGTCTGAAGGA; *HPRT1* Fw GTCTTGCTCGAGATGTGATG and *HPRT1* Rw GTAATCCAGCAGGTCAGCAA. Target transcripts were analyzed with the QuantStudio 7 System (Applied Biosystems, CA, USA). The comparative threshold cycle (Ct) method was used for quantification analysis. The Ct values of each gene were normalized to the Ct value of HPRT1. The gene expression levels were evaluated by the fold change using the equation 2-ΔΔCt.

HLA *sequencing*

HLA-class I and *II* genes were targeted for DNA sequencing using a biotinylated DNA probe-based capture method [50], with modifications as follows. Genomic DNA (500 ng from each sample) was fragmented enzymatically using the NEBNext Ultra ii FS module (New England Biolabs, E7810S). Individual samples were labeled uniquely using 3 μl of 15 μM custom dual-index adapters (Integrated DNA Technologies, Coralville, IA, USA) and the NEB ligation module. Post ligation cleanup was based on the Kapa Hyper Prep protocol (Kapa Biosystems, Wilmington, MA) and followed by dual size selection. Paired ends of 250 bp each were sequenced using a NovaSeq instrument and SP Reagent Kit (Illumina Inc, San Diego, CA, USA). *HLA* alleles were determined from the sequence data using the consensus from three algorithms: NGSengine 2.10.0 (GenDX, Utrecht, The Netherlands), HLA Twin (Omixon Biocomputing Ltd. Budapest, Hungary) and HLA*LA [51].

ORCID

Stefania Mantovani http://orcid.org/0000-0002-5885-2842
Ottavia Spiga http://orcid.org/0000-0002-0263-7107
Andrea M. Isidori http://orcid.org/0000-0002-9037-5417
Mario U Mondelli http://orcid.org/0000-0003-1811-3153
Alessandra Renieri http://orcid.org/0000-0002-0846-9220

References

[1] Lee IH, Lee JW, Kong SW. A survey of genetic variants in SARS-CoV-2 interacting domains of ACE2, TMPRSS2 and TLR3/7/8 across populations. Infect Genet Evol. 2020;85:104507.

[2] Mukherjee S, Huda S, Sinha Babu SP. Toll-like receptor polymorphism in host immune response to infectious diseases: a review. Scand J Immunol. 2019 Jul;90(1):e12771.

[3] Perales-Linares R, Navas-Martin S. Toll-like receptor 3 in viral pathogenesis: friend or foe? Immunology. Immunology. 2013 Oct;140(2):153–167.

[4] Totura AL, Whitmore A, Agnihothram S, et al. Toll-Like receptor 3 signaling via TRIF contributes to a protective innate immune response to severe acute respiratory syndrome coronavirus infection. mBio 2015 May 26;6(3):e00638–15.

[5] Matsumoto M, Oshiumi H, Seya T. Antiviral responses induced by the TLR3 pathway. Rev Med Virol. 2011 Mar;21(2):67–77.

[6] Schulz O, Diebold SS, Chen M, et al. Toll-like receptor 3 promotes cross-priming to virus-infected cells. Nature. 2005 Feb 24;433 (7028):887–892.

[7] Suresh MV, Dolgachev VA, Zhang B, et al. TLR3 absence confers increased survival with improved macrophage activity against pneumonia. JCI Insight. 2019 Dec 5;4(23):e131195.

[8] Ranjith-Kumar CT, Miller W, Sun J, et al. Effects of single nucleotide polymorphisms on Toll-Like receptor 3 activity and expression in cultured cells. J Biol Chem. 2007 Jun 15;282(24):17696–17705.

[9] Teimouri H, Maali A. Single-nucleotide polymorphisms in host pattern-recognition receptors show association with antiviral responses against SARS-CoV-2, in-silico trial. JoMMID. 2020;8 (2):65–70.

[10] Dhangadamajhi G, Rout R, Cavazos-Escobar E. Association of TLR3 functional variant (rs3775291) with COVID-19 susceptibility and death: a population-scale study. Hum Cell. 2021 Feb 22;34:1–3.

[11] Franco LH, Fleuri AKA, Pellison NC, et al. Autophagy downstream of endosomal Toll-Like receptor signaling in macrophages is a key mechanism for resistance to Leishmania major infection. J Biol Chem. 2017 Aug 11;292(32):13087–13096.

[12] Kirkin V, McEwan DG, Novak I, et al. A role for ubiquitin in selective autophagy. Mol Cell. 2009 May 15;34(3):259–269.

[13] Delgado MA, Elmaoued RA, Davis AS, et al. Toll-like receptors control autophagy. EMBO J. 2008 Apr 9;27(7):1110–1121.

[14] Levine B, Mizushima N, Virgin HW. Autophagy in immunity and inflammation. Nature. 2011 Jan 20;469(7330):323–335.

[15] Prentice E, Jerome WG, Yoshimori T, et al. Coronavirus replication complex formation utilizes components of cellular autophagy. J Biol Chem. 2004 Mar 12;279(11):10136–10141.

[16] Guo L, Yu H, Gu W, et al. Autophagy negatively regulates transmissible gastroenteritis virus replication. Sci Rep. 2016 Mar 31;6: 23864.

[17] Carvalho-Schneider C, Laurent E, Lemaignen A, et al. Follow-up of adults with noncritical COVID-19 two months after symptom onset. Clin Microbiol Infect. 2021 Feb;27(2):258–263.

[18] Hoffmann M, Kleine-Weber H, Schroeder S, et al. SARS-CoV-2 cell entry depends on ACE2 and TMPRSS2 and is blocked by a clinically proven protease inhibitor. Cell. 2020Apr16;181 (2):271–280.e8.

[19] Miao Y, Fan L, Li JY. Potential treatments for COVID-19 related cytokine storm - beyond corticosteroids. Front Immunol. 2020 Jun 16;11: 1445.

[20] Shojaei S, Suresh M, Klionsky DJ, et al. Autophagy and SARS-CoV-2 infection: a possible smart targeting of the autophagy pathway. Virulence. 2020 Dec;11(1):805–810.

[21] Benvenuto D, Angeletti S, Giovanetti M, et al. Evolutionary analysis of SARS-CoV-2: how mutation of non-structural protein 6 (NSP6) could affect viral autophagy. J Infect. 2020 Jul;81(1):e24–e27.

[22] Jamwal S, Gautam A, Elsworth J, et al. An updated insight into the molecular pathogenesis, secondary complications and potential therapeutics of COVID-19 pandemic. Life Sci. 2020 Sep 15;257: 118105.

[23] Torcia MG, Nencioni L, Clemente AM, et al. Sex differences in the response to viral infections: TLR8 and TLR9 ligand stimulation induce higher IL10 production in males. PLoS One. 2012;7 (6):e39853.

[24] Lim HK, Huang SXL, Chen J, et al. Severe influenza pneumonitis in children with inherited TLR3 deficiency. J Exp Med. 2019 Sep 2;216(9):2038–2056.

[25] Zhang Q, Bastard P, Liu Z, et al. Inborn errors of type I IFN immunity in patients with life-threatening COVID-19. Science. 2020 Oct 23;370(6515):eabd4570.

[26] Enkhbayar P, Kamiya M, Osaki M, et al. Structural principles of leucine-rich repeat (LRR) proteins. Proteins. 2004 Feb 15;54 (3):394–403.

[27] Rothberg JM, Jacobs JR, Goodman CS, et al. slit: an extracellular protein necessary for development of midline glia and commissural axon pathways contains both EGF and LRR domains. Genes Dev. 1990 Dec;4(12A):2169–2187.

[28] Kobe B, Kajava AV. The leucine-rich repeat as a protein recognition motif. Curr Opin Struct Biol. 2001 Dec;11(6):725–732.

[29] Gao T, Zhang SP, Wang JF, et al. TLR3 contributes to persistent autophagy and heart failure in mice after myocardial infarction. J Cell Mol Med. 2018 Jan;22(1):395–408.

[30] Mehra MR, Ruschitzka F, Patel AN. Retraction-Hydroxychloroquine or chloroquine with or without a macrolide for treatment of COVID-19: a multinational registry analysis. Lancet. 2020 Jun 13;395(10240):1820.

[31] Mahase E. Covid-19: WHO halts hydroxychloroquine trial to review links with increased mortality risk. BMJ 2020 May 28;369: m2126.

[32] Ayele Mega T, Feyissa TM, Dessalegn Bosho D, et al. The outcome of hydroxychloroquine in patients treated for COVID-19: systematic review and meta-analysis. Can Respir J. 2020 Oct 13;2020: 4312519.

[33] Klionsky DJ, Abdel-Aziz AK, Abdelfatah S, et al. Guidelines for the use and interpretation of assays for monitoring autophagy (4th edition). Autophagy 2021 Feb;8:1–382.

[34] Levy JMM, Towers CG, Thorburn A. Targeting autophagy in cancer. Nat Rev Cancer. 2017 Sep;179:528–542. [Epub 2017 Jul 28]. PMID: 28751651; PMCID: PMC5975367.

[35] Michalakis K, Ilias I. SARS-CoV-2 infection and obesity: common inflammatory and metabolic aspects. Diabetes Metab Syndr. 2020 Jul-Aug;14(4):469–471.

[36] Vomero M, Barbati C, Colasanti T, et al. Autophagy modulation in lymphocytes from COVID-19 patients: new therapeutic target in SARS-COV-2 infection. Front Pharmacol. 2020 Nov 19;11: 569849.

[37] Jang CH, Choi JH, Byun MS, et al. Chloroquine inhibits production of TNF-alpha, IL-1beta and IL-6 from lipopolysaccharide-stimulated human monocytes/macrophages by different modes. Rheumatology (Oxford). 2006 Jun;45 (6):703–710.

[38] Hayn M, Hirschenberger M, Koepke L, et al. Systematic functional analysis of SARS-CoV-2 proteins uncovers viral innate immune antagonists and remaining vulnerabilities. Cell Rep. 2021 May 18;357:109126. [Epub 2021 Apr 27]. PMID: 33974846; PMCID: PMC8078906.

[39] Nahum A, Dadiac H, Batesac A, et al. The biological significance of TLR3 variant, L412F, in conferring susceptibility to cutaneous candidiasis, CMV and autoimmunity. Autoimmun Rev. 2012 Mar;11(5):341–347.

[40] Aslaksen S, Wolff AB, Vigeland MD, et al. Identification and characterization of rare toll-like receptor 3 variants in patients with autoimmune Addison's disease. J Transl Autoimmun. 2019 May 28;1:100005.

[41] Wu DJ, Adamopoulos IE. Autophagy and autoimmunity. Clin Immunol. 2017Mar;176:55–62.

[42] Caza TN, Talaber G, Perl A. Metabolic regulation of organelle homeostasis in lupus T cells. Clin Immunol. 2012 Sep;144 (3):200–213.

[43] Keller CW, Lünemann JD. Autophagy and autophagy-related proteins in CNS autoimmunity. Front Immunol. 2017 Feb 27;8: 165.

[44] De Sousa E, Ligeiro D, Lérias JR, et al. Mortality in COVID-19 disease patients: correlating the association of major histocompatibility complex (MHC) with severe acute respiratory syndrome 2 (SARS-CoV-2) variants. Int J Infect Dis. 2020 Sep;98:454–459. Epub 2020 Jul 18.

[45] Erichsen MM, Løvås K, Skinningsrud B, et al. Clinical, immunological, and genetic features of autoimmune primary adrenal insufficiency: observations from a Norwegian registry. J Clin Endocrinol Metab. 2009 Dec;94(12):4882–4890.

[46] Smigoc Schweiger D, Mendez A, Kunilo Jamnik S, et al. High-risk genotypes HLA-DR3-DQ2/DR3-DQ2 and DR3-DQ2/DR4-DQ8 in co-occurrence of type 1 diabetes and celiac disease. Autoimmunity. 2016 Jun;49(4):240–247.

[47] Daga S, Fallerini C, Baldassarri M, et al. Employing a systematic approach to biobanking and analyzing clinical and genetic data for advancing COVID-19 research. Eur J Hum Genet. 2021 Jan;17:1–15.

[48] Molnar R. Interpretable machine learning. A guide for making black box models explainable. 2020. lulu.com.

[49] Tibshirani R. Regression shrinkage and selection via the Lasso. Journal of the Royal Statistical Society: Series B (Methodological). 1996;58(1):267–288.

[50] Norman PJ, Hollenbach JA, Nemat-Gorgani N, et al. Defining KIR and HLA Class I genotypes at highest resolution via high-throughput sequencing. Am J Hum Genet. 2016 Aug 4;99 (2):375–391.

[51] Dilthey AT, Mentzer AJ, Carapito R, et al. HLA*LA-HLA typing from linearly projected graph alignments. Bioinformatics. 2019 Nov 1;35(21):4394–4396.

GEN-COVID Multicenter Study (https://sites.google.com/dbm.unisi.it/gen-covid)

Mirella Bruttini[1,2,17], Rossella Tita[17], Sara Amitrano[17], Anna Maria Pinto[17], Maria Antonietta Mencarelli[17], Caterina Lo Rizzo[17], Valentina Perticaroli[1,2,17], Massimiliano Fabbiani[19], Barbara Rossetti[19], Giacomo Zanelli[2,19], Elena Bargagli[20], Laura Bergantini[20], Miriana D'Alessandro[20], Paolo Cameli[20], David Bennett[20], Federico Anedda[21], Simona Marcantonio[21], Sabino Scolletta[21], Federico Franchi[21], Maria Antonietta Mazzei[22], Susanna Guerrini[22], Edoardo Conticini[23], Luca Cantarini[23], Bruno Frediani[23], Danilo Tacconi[24], Chiara Spertilli[24], Marco Feri[25], Alice Donati[25], Raffaele Scala[26], Luca Guidelli[26], Genni Spargi[27], Marta Corridi[27], Cesira Nencioni[28], Leonardo Croci[28], Gian Piero Caldarelli[29], Maurizio Spagnesi[30], Paolo Piacentini[30], Maria Bandini[30], Elena Desanctis[30], Silvia Cappelli[30], Anna Canaccini[31], Agnese Verzuri[31], Valentina Anemoli[31], Agostino Ognibene[32], Alessandro Pancrazzi[32], Maria Lorubbio[32], Massimo Vaghi[33], Antonella D'Arminio Monforte[34], Esther Merlini[34], Federica Gaia Miraglia[34], Raffaele Bruno[35,36], Marco Vecchia[35], Serena Ludovisi[37], Massimo Girardis[38], Sophie Venturelli[38], Marco Sita[38], Andrea Cossarizza[39], Andrea Antinori[40], Alessandra Vergori[40], Arianna Emiliozzi[40], Stefano Rusconi[41,42], Matteo Siano[42], Arianna Gabrieli[42], Agostino Riva[41,42], Daniela Francisci[4344], Elisabetta Schiaroli[4344], Francesco Paciosi[44], Pier Giorgio Scotton[45], Francesca Andretta[45], Sandro Panese[45], Renzo Scaggiante[47], Francesca Gatti[48], Saverio Giuseppe Parisi[48], Melania degli Antoni[49], Isabella Zanella[51,41], Matteo Della Monica[52], Carmelo Piscopo[52], Mario Capasso[53,54,55], Roberta Russo[53,54], Immacolata Andolfo[53,54], Achille Iolascon[53,54], Giuseppe Fiorentino[55], Massimo Carella[56], Marco Castori[56], Filippo Aucella[57], Pamela Raggi[58], Carmen Marciano[58], Rita Perna[58], Matteo Bassetti[59,60], Antonio Di Biagio[59,60], Maurizio Sanguinetti[61,62], Luca Masucci[61,62], Serafina Valente[63], Marco Mandalà[64], Alessia Giorli[64], Lorenzo Salerni[64], Patrizia Zucchi[65], Pierpaolo Parravicini[65], Elisabetta Menatti[66] Stefano Baratti[45], Tullio Trotta[67], Ferdinando Giannattasio[67], Gabriella Coiro[67], Fabio Lena[68], Domenico A. Coviello[69], Cristina Mussini[70], Giancarlo Bosio[71], Enrico Martinelli[71], Sandro Mancarella[72], Luisa Tavecchia[72], Mary Ann Belli[72], Lia Crotti[73,74,75,76], Gianfranco Parati[73,74], Marco Gori[77,78], Maurizio Sanarico[79], Stefano Ceri[80], Pietro Pinoli[80], Francesco Raimondi[81], Filippo Biscarini[82], Alessandra Stella[82], Marco Rizzi[83], Franco Maggiolo[83], Diego Ripamonti[83], Claudia Suardi[84], Tiziana Bachetti[85], Maria Teresa La Rovere[86], Simona Sarzi-Braga[87], Maurizio Bussotti[88], Katia Capitani[2,89], Kristina Zguro[2], Simona Dei[90], Sabrina Ravaglia[91], Rosangela Artuso[92], Antonio Perrella[93], Francesco Bianchi[2,93], Giuseppe Merla[53,94], Gabriella Maria Squeo[94], Mario Tumbarello[2,19], Ilaria Rancan[2,19], Davide Romani[30], Manola Pisani[31], Stefano Busani[43], Andrea Tommasi[43], Francesco Castelli[49], Eugenia Quiros-Roldan[49], Alessandra Guarnaccia[61], Oreste De Vivo[63], Gabriella Doddato[1,2], Annarita Giliberti[1,2], Francesca Ariani[1,2,17], Gianluca Lacerenza[95], Elena Andreucci[92], Giulia Gori[92], Angelica Pagliazzi[92], Erika Fiorentini[92], Paola Bergomi[96], Emanuele Catena[96], Riccardo Colombo[96], Sauro Luchi[97], Giovanna Morelli[97], Paola Petrocelli[97], Sarah Iacopini[97], Sara Modica[97], Silvia Baroni[98], Francesco Vladimiro Segala[99], Francesco Menichetti[100], Marco Falcone[100], Giusy Tiseo[100], Chiara Barbieri[100], Tommaso Matucci[100], Davide Grassi[101], Claudio Ferri[101], Franco Marinangeli[102], Francesco Brancati[103], Antonella Vincenti[104], Valentina Borgo[104], Lombardi Stefania[104], Mirco Lenzi[104], Massimo Antonio Di Pietro[105], Francesca Vichi[105], Benedetta Romanin[105], Letizia Attala[105], Cecilia Costa[105], Andrea Gabbuti[105], Menè Roberto[106], Umberto Zuccon[107], Lucia Vietri[107], Patrizia Casprini[108], Marcello Maffezzoni[109] and Marta Colaneri[110]

[19]Department of Medical Sciences, Infectious and Tropical Diseases Unit, Azienda Ospedaliera Universitaria Senese, Siena, Italy
[20]Respiratory Diseases Unit, Department of Medicine, Surgery and Neurosciences, Siena University Hospital, Siena, Italy
[21]Department of Emergency and Urgency, Medicine, Surgery and Neurosciences, Unit of Intensive Care Medicine, Siena University Hospital, Italy
[22]Department of Medical, Surgical and Neurosciences and Radiological Sciences, Unit of Diagnostic Imaging, University of Siena
[23]Rheumatology Unit, Department of Medicine, Surgery and Neurosciences, University of Siena, Policlinico Le Scotte, Italy
[24]Department of Specialized and Internal Medicine, Infectious Diseases Unit, San Donato Hospital Arezzo, Italy
[25]Department of Emergency, Anesthesia Unit, San Donato Hospital, Arezzo, Italy
[26]Department of Specialized and Internal Medicine, Pneumology Unit and UTIP, San Donato Hospital, Arezzo, Italy
[27]Department of Emergency, Anesthesia Unit, Misericordia Hospital, Grosseto, Italy
[28]Department of Specialized and Internal Medicine, Infectious Diseases Unit, Misericordia Hospital, Grosseto, Italy
[29]Clinical Chemical Analysis Laboratory, Misericordia Hospital, Grosseto, Italy
[30]Department of Preventive Medicine, Azienda USL Toscana Sud Est, Italy
[31]Territorial Scientific Technician Department, Azienda USL Toscana Sud Est, Italy
[32]Laboratory Medicine Department, San Donato Hospital, Arezzo, Italy
[33]Chirurgia Vascolare, Ospedale Maggiore di Crema, Italy
[34]Department of Health Sciences, Clinic of Infectious Diseases, ASST Santi Paolo e Carlo, University of Milan, Italy

[35]Division of Infectious Diseases and Immunology, Fondazione IRCCS Policlinico San Matteo, Pavia, Italy

[36]Department of Internal Medicine and Therapeutics, University of Pavia, Italy

[37]Fondazione IRCCS Ca' Granda Ospedale Maggiore Policlinico, Milano, Italy

[38]Department of Anesthesia and Intensive Care, University of Modena and Reggio Emilia, Modena, Italy

[39]Department of Medical and Surgical Sciences for Children and Adults, University of Modena and Reggio Emilia, Modena, Italy

[40]HIV/AIDS Department, National Institute for Infectious Diseases, IRCCS, Lazzaro Spallanzani, Rome, Italy

[41]III Infectious Diseases Unit, ASST-FBF-Sacco, Milan, Italy

[42]Department of Biomedical and Clinical Sciences Luigi Sacco, University of Milan, Milan, Italy

[43]Infectious Diseases Clinic, Department of Medicine , University of Perugia, Santa Maria della Misericordia Hospital, Perugia, Italy

[44]

[45]Department of Infectious Diseases, Treviso Hospital, Local Health Unit 2 Marca Trevigiana, Treviso, Italy

[46]Clinical Infectious Diseases, Mestre Hospital, Venezia, Italy.

[47]Infectious Diseases Clinic, ULSS1, Belluno, Italy

[48]Department of Molecular Medicine, University of Padova, Italy

[49]Department of Infectious and Tropical Diseases, University of Brescia and ASST Spedali Civili Hospital, Brescia, Italy

[50]Department of Molecular and Translational Medicine, University of Brescia, Italy;

[51]Clinical Chemistry Laboratory, Cytogenetics and Molecular Genetics Section, Diagnostic Department, ASST Spedali Civili di Brescia, Italy

[52]Medical Genetics and Laboratory of Medical Genetics Unit, A.O.R.N. "Antonio Cardarelli", Naples, Italy

[53]Department of Molecular Medicine and Medical Biotechnology, University of Naples Federico II, Naples, Italy

[54]CEINGE Biotecnologie Avanzate, Naples, Italy

[55]Unit of Respiratory Physiopathology, AORN dei Colli, Monaldi Hospital, Naples, Italy

[56]Division of Medical Genetics, Fondazione IRCCS Casa Sollievo della Sofferenza Hospital, San Giovanni Rotondo, Italy

[57]Department of Medical Sciences, Fondazione IRCCS Casa Sollievo della Sofferenza Hospital, San Giovanni Rotondo, Italy

[58]Clinical Trial Office, Fondazione IRCCS Casa Sollievo della Sofferenza Hospital, San Giovanni Rotondo, Italy

[59]Department of Health Sciences, University of Genova, Genova, Italy

[60]Infectious Diseases Clinic, Policlinico San Martino Hospital, IRCCS for Cancer Research Genova, Italy

[61]Microbiology, Fondazione Policlinico Universitario Agostino Gemelli IRCCS, Catholic University of Medicine, Rome, Italy

[62]Department of Laboratory Sciences and Infectious Diseases, Fondazione Policlinico Universitario A. Gemelli IRCCS, Rome, Italy

[63]Department of Cardiovascular Diseases, University of Siena, Siena, Italy

[64]Otolaryngology Unit, University of Siena, Italy

[65]Department of Internal Medicine, ASST Valtellina e Alto Lario, Sondrio, Italy

[66]Study Coordinator Oncologia Medica e Ufficio Flussi, Sondrio, Italy

[67]First Aid Department, Luigi Curto Hospital, Polla, Salerno, Italy

[68]Local Health Unit-Pharmaceutical Department of Grosseto, Toscana Sud Est Local Health Unit, Grosseto, Italy

[69]U.O.C. Laboratorio di Genetica Umana, IRCCS Istituto G. Gaslini, Genova, Italy.

[70]Infectious Diseases Clinics, University of Modena and Reggio Emilia, Modena, Italy.

[71]Department of Respiratory Diseases, Azienda Ospedaliera di Cremona, Cremona, Italy

[72]U.O.C. Medicina, ASST Nord Milano, Ospedale Bassini, Cinisello Balsamo (MI), Italy

[73]Istituto Auxologico Italiano, IRCCS, Department of Cardiovascular, Neural and Metabolic Sciences, San Luca Hospital, Milan, Italy

[74]Department of Medicine and Surgery, University of Milano-Bicocca, Milan, Italy

[75]Istituto Auxologico Italiano, IRCCS, Center for Cardiac Arrhythmias of Genetic Origin, Milan, Italy

[76]Istituto Auxologico Italiano, IRCCS, Laboratory of Cardiovascular Genetics, Milan, Italy

[77]University of Siena, Diism-sailab, Siena, Italy

[78]University Cote d'Azur, Inria, CNRS, I3S, Maasai

[79]Independent Data Scientist, Milan, Italy

[80]Department of Electronics, Information and Bioengineering (DEIB), Politecnico di Milano, Milano, Italy

[81]Scuola Normale Superiore, Pisa, Italy

[82]CNR-Consiglio Nazionale delle Ricerche, Istituto di Biologia e Biotecnologia Agraria (IBBA), Milano, Italy

[83]Unit of Infectious Diseases, ASST Papa Giovanni XXIII Hospital, Bergamo, Italy

[84]Fondazione per la ricerca Ospedale di Bergamo, Bergamo, Italy

[85]Direzione Scientifica, Istituti Clinici Scientifici Maugeri IRCCS, Pavia, Italy

[86]Istituti Clinici Scientifici Maugeri IRCCS, Department of Cardiology, Institute of Montescano, Pavia, Italy

[87]Istituti Clinici Scientifici Maugeri, IRCCS, Department of Cardiac Rehabilitation, Institute of Tradate (VA), Italy

[88]Istituti Clinici Scientifici Maugeri IRCCS, Department of Cardiology, Institute of Milan, Milan, Italy

[89]IRCCS C. Mondino Foundation, Pavia, Italy

[90]Core Research Laboratory, ISPRO, Florence, Italy

[91]Health Management, Azienda USL Toscana Sudest, Tuscany, Italy

[92]Medical Genetics Unit, Meyer Children's University Hospital, Florence, Italy

[93]Department of Medicine, Pneumology Unit, Misericordia Hospital, Grosseto, Italy

[94]Laboratory of Regulatory and Functional Genomics, Fondazione IRCCS Casa Sollievo della Sofferenza, San Giovanni Rotondo (Foggia), Italy

[95]Department of Pharmaceutical Medicine, Misericordia Hospital, Grosseto, Italy

[96]Department of Anesthesia and Intensive Care Unit, ASST Fatebenefratelli Sacco, Luigi Sacco Hospital, Polo Universitario, University of Milan, Milan, Italy

[97]Infectious Disease Unit, Hospital of Lucca, Lucca, Italy

[98]Department of Diagnostic and Laboratory Medicine, Unity of Chemistry, Biochemistry and Clinical Molecular Biology, Fondazione Policlinico Universitario A. Gemelli IRCCS, Catholic University of the Sacred Heart, Rome, Italy

[99]Clinic of Infectious Diseases, Catholic University of the Sacred Heart, Rome, Italy

[100]Department of Clinical and Experimental Medicine, Infectious Diseases Unit, University of Pisa, Pisa, Italy

[101]Department of Clinical Medicine, Public Health, Life and Environment Sciences, University of L'Aquila, L'Aquila, Italy

[102]Anesthesiology and Intensive Care, University of L'Aquila, L'Aquila, Italy

[103]Medical Genetics Unit, Department of Life, Health and Environmental Sciences, University of L'Aquila, L'Aquila, Italy

[104]Infectious Disease Unit, Hospital of Massa, Massa Carrara, Italy

[105]Unit of Infectious Diseases, S.M. Annunziata Hospital, Florence, Italy

[106]Istituto Auxologico Italiano, IRCCS, Department of Cardiovascular, Neural and Metabolic Sciences, San Luca Hospital; Department of Medicine and Surgery, University of Milano-Bicocca, Milan, Italy

[107]Respiratory Diseases Unit, "Santa Maria degli Angeli" Hospital, Pordenone, Italy

[108]Laboratory of Clinical Pathology and Immunoallergy, Florence-Prato, Italy

[109]University of Pavia, Pavia, Italy

[110]Division of Infectious Diseases I, Fondazione IRCCS Policlinico San Matteo, Pavia, Italy